Study of the QCD phase diagram with a nonzero chiral chemical potential

V. V. Braguta*

Institute for High Energy Physics NRC "Kurchatov Institute", Protvino 142281, Russia; Institute of Theoretical and Experimental Physics, 117259 Moscow, Russia; Far Eastern Federal University, School of Natural Sciences, 690950 Vladivostok, Russia; and Moscow Institute of Physics and Technology, Dolgoprudny 141700, Russia

E.-M. Ilgenfritz†

Joint Institute for Nuclear Research, BLTP, 141980 Dubna, Russia

A. Yu. Kotov‡

Institute of Theoretical and Experimental Physics, 117259 Moscow, Russia; and National Research Nuclear University MEPhI (Moscow Engineering Physics Institute), Moscow 115409, Russia

B. Petersson§

Humboldt-Universität zu Berlin, Institut für Physik, 12489 Berlin, Germany

S. A. Skinderev‖

Institute of Theoretical and Experimental Physics, 117259 Moscow, Russia

(Received 15 January 2016; published 25 February 2016)

In this paper we report on lattice simulations of $SU(3)$–QCD with nonzero chiral chemical potential. We focus on the influence of the chiral chemical potential on the confinement/deconfinement phase transition and the breaking/restoration of chiral symmetry. The simulation is carried out with dynamical Wilson fermions. We find that the critical temperature rises as the chiral chemical potential grows.

DOI: 10.1103/PhysRevD.93.034509

I. INTRODUCTION

The aim of relativistic heavy ion collisions is to study the phase structure of QCD in a more or less unknown region and to explore exotic properties of the phases becoming accessible at high densities of energy and baryonic number. Understanding the interplay of strong electromagnetic fields with the basic mechanisms of QCD has turned out as a similarly interesting direction of research since 2008 [1], although not primarily targeted as the high matter density itself, which is characterized by the baryonic chemical potential μ_B. This interplay, in particular in the quark-gluon phase, makes its study even more interesting. Here the chiral chemical potential μ_5 is of central importance.

Indeed, in noncentral collisions the strongest magnetic fields on Earth ($qB \sim \mathcal{O}(1..15)m_\pi^2$) are created [2] at the Relativistic Heavy Ion Collider and LHC with a lifetime of few fm$/c$ in each collision. There exist also electric field fluctuations of a similar order of magnitude [3]. If electric and magnetic fields are coupled through the Ohmic and anomalous conductivities of the plasma, the magnetic field due to the spectators is practically unaltered [4].

The coupling between color and electromagnetic fields belongs to the field of phenomena possible due to the axial anomaly [5–7]. Besides the well-known role it is playing in the QCD vacuum at $T = 0$, it has a constitutive role under the extremal conditions which exist in the intermediate nonhadronic phase as well as in certain condensed matter systems [8] as recently has been noticed.

The violation of $U_A(1)$ symmetry (which is not spontaneously broken but rather due to the topological vacuum structure at $T = 0$) is well known in the form of mass splittings between hadrons [9,10] (and signalled by further observables like $\Delta = \langle\pi\pi\rangle - \langle\delta\delta\rangle$, the splitting between the π and δ norms, the T dependence of the Dirac spectral density, and of the topological susceptibility χ_{top}). The $U_A(1)$ symmetry will be restored in the temperature range up to few times T_c. How this happens in detail in real QCD in contrast to pure Yang-Mills theory [11] is under intensive study on the lattice [12–17].

Instead of topological charge appearing (at the infrared scale) in the form of Euclidean instantons or dyons [18]), the axial anomaly will play a dynamical role during the short time of the existence of liberated quarks. Mesoscopic domains of (almost classical) strongly CP violating gluon fields are created during the initial stadium

*braguta@itep.ru
†ilgenfri@theor.jinr.ru
‡kotov@itep.ru
§bengt@physik.hu-berlin.de
‖sergeant.mipt@mail.ru

of a collision (with a color electric and magnetic fields $\vec{E}^a \| \vec{B}^a \|$collision axis). This is believed to lead to the accumulation of a chiral imbalance between quarks, $n_5 = n(\text{lefthanded}) - n(\text{righthanded}) \neq 0$ (with random sign and strength). The analogon of instanton tunneling at high temperature, the sphaleron transitions over the barrier (frequent at $T > T_c$), give rise to a Chern-Simons diffusion rate $\Gamma \propto T^4$) which is insufficient to completely wash out the chiral imbalance existing during the lifetime of the high-temperature phase. This, together with the magnetic field $\vec{B}$ mentioned before, gives rise to the anomalous transport of electric current along the magnetic field (the so-called chiral magnetic effect; for a recent report see Ref. [19]), as a remnant of the temporal and local violation of P and CP invariance). Thus, a charge asymmetry with respect to the collision plane remains as an effect of the electric current $\vec{J} \propto \mu_5 \vec{H}$ flowing while the deconfined phase has existed. This is the crucial role of μ_5. One can also note other phenomena in media with a chiral imbalance [20,21].

Of course, a precise scenario has to be the result of a space-time transport simulation. In an intermediate step, lattice QCD should explore the multidimensional phase diagram, including (beyond temperature) one or two chemical potentials (baryonic μ_B and/or μ_5) and the magnetic field strength. In a first generation of lattice studies, the effect of an external magnetic field on the temperature of the chiral and/or deconfining transition has been studied [22–24] in isolation. This has led to the discovery of the interplay of opposite tendencies (magnetic catalysis and inverse catalysis of the chiral condensate) at different temperatures. The phase diagram of QCD in a magnetic field has been reviewed in Ref. [25].

Baryonic density $n_B = (n(\text{quarks}) - n(\text{antiquarks}))/3$, modelled by $\mu_B \neq 0$, still remains difficult to simulate (if not $\mu_B \ll T$) except for $SU(2)$. For this model system a simulation with $N_f = 2$ flavors of staggered fermions has been recently performed [26,27], following earlier work for $SU(2)$ (with Wilson fermions) which has been summarized in Ref. [28]. Chiral imbalance, however, $n_5 = n(\text{lefthanded}) - n(\text{righthanded}) \neq 0$ (expected in the result of the chiral anomaly), can be modelled by a chiral chemical potential μ_5 without a sign problem. It would be very interesting to study the simultaneous influence of magnetic field and chiral imbalance on the transition temperature. In such studies, as soon as a magnetic field $\vec{H}$ is included, the induced electric current $\vec{J} \propto \mu_5 \vec{B}$ would be among the most interesting observables as proposed in Ref. [29].

In a few recent papers [30,31], our collaboration has begun to study the effect of nonvanishing chiral chemical potential μ_5 on the transition temperature. We did this first for two-color Yang-Mills theory coupled to staggered fermions without rooting (four flavors). With the present paper we report our results obtained within an extension of our codes to $SU(3)$ Yang-Mills theory coupled to two flavors of Wilson fermions. Preliminary results have been already reported at Lattice Symposium 2015.

Section II is devoted to the details of the calculation. In Sec. III we present our results, and in Sec. IV we discuss them. In the Appendix we study renormalization properties of the chiral condensate with nonzero chiral chemical potential.

II. DETAILS OF THE SIMULATION

In the simulation we used the $SU(3)$ one-plaquette gauge action and a Wilson fermionic action with two degenerate quark flavors. The Dirac operator with nonzero chiral chemical potential has the form [32]

$$\begin{aligned} D_{xy} = 1 - \kappa \sum_i ((1-\gamma_i)U_i(x)\delta_{x+i,y} + (1+\gamma_i)U_i^\dagger(y)\delta_{x-i,y}) \\ - \kappa((1-\gamma_4 e^{\mu_5 a \gamma_5})U_4(x)\delta_{x+4,y} \\ + (1+\gamma_4 e^{-\mu_5 a\gamma_5})U_4^\dagger(y)\delta_{x-4,y}). \end{aligned} \tag{1}$$

Here μ_5 enters through an additional exponential factor for timelike link variables. In the naive continuum limit $a \to 0$, the fermion action with the Dirac operator (1) corresponds to the fermion action with a chiral chemical potential (mass and hopping parameter are related as $\kappa = \frac{1}{2ma+8}$):

$$S_f^{(\text{cont})} = \int d^4x \bar{\psi}(\partial_\mu \gamma_\mu + igA_\mu\gamma_\mu + m + \mu_5\gamma_5\gamma_4)\psi. \tag{2}$$

The Wilson Dirac operator (1) is γ_5-Hermitian:

$$\gamma_5 D^\dagger(\mu_5)\gamma_5 = D(\mu_5). \tag{3}$$

This property implies that its determinant $\det D(\mu_5)$ is real, and in the case of $N_f = 2$ fermion flavors it is positive. Thus, the system has no sign problem and can be simulated by standard hybrid Monte Carlo methods.

In our simulations we used Wilson fermions since they allow the introduction of the chiral chemical potential μ_5 in a local exponential form, which is not possible for staggered fermions. Moreover, calculations with dynamical Wilson fermions require less computational resources.

We have performed simulations on a lattice 4×16^3, with $\kappa = 0.1665$ kept fixed throughout the simulations (performed as a β-scan). For $\beta = 5.32144$ (in the transition region) the chosen κ corresponds to a lattice step size $a = 0.13$ fm and to a pion mass $m_\pi = 418$ MeV. Our measured observables are the Polyakov loop, the chiral condensate, and their respective susceptibilities. The Polyakov loop and its susceptibility are sensitive to the confinement/deconfinement transition, while the chiral condensate and its susceptibility are sensitive to the chiral symmetry breaking/restoration aspects. We present the observables as functions of β for our scans at four different values of $\mu_5 a = 0.0$, 0.25, 0.5, 0.75.

III. RESULTS OF THE SIMULATION

In Fig. 1 we show the Polyakov loop and the chiral condensate as functions of β for various $\mu_5 a$. The sharp change of observables indicates the position of the phase transition. One clearly sees that nonzero chiral chemical potential shifts both phase transitions to larger values of β. This means that the transition temperatures increases with μ_5. A splitting between both phase transitions is not observed.

In order to confirm our observation and to better identify the transition point we also have measured the chiral susceptibility and the Polyakov loop susceptibility as functions of β. The results are presented in Fig. 2. The peak positions of the susceptibilities correspond to the positions of the respective transition. From these observables one can now definitely conclude that the critical temperature grows with increasing μ_5.

In order to determine the critical temperatures we fitted the plots for the susceptibilities with a Gaussian function: $f(\beta) = a_0 + a_1 e^{-(\beta-\beta_c)^2/\sigma^2}$ (we used six to seven points near the peak). The dependence of the critical β_c extracted from the fit is shown in Fig. 3. For both susceptibilities it can be described by a quadratic fit:

$$\beta_c = 5.18 + 0.12(\mu_5 a)^2. \tag{4}$$

Using the two-loop β-function, we extract the dependence of the critical temperature on $\mu_5 a$. The resulting phase diagram is presented in Fig. 4.

At the end of this section it is important to discuss the ultraviolet divergences of the chiral condensate and of the Polyakov loop and how they affect our results. In Ref. [31] it was shown that the introduction of a nonzero chiral chemical potential for staggered fermions leads to an additional logarithmic divergence in the chiral condensate $\sim\mu_5^2 \log(a)$, whereas it does not lead to an additional divergence in the Polyakov loop. In the present work we perform simulations with Wilson fermions, and it is important to study the ultraviolet divergences which appear in the observables in the case of Wilson fermions. First one can repeat all steps in the derivation presented in Ref. [31]

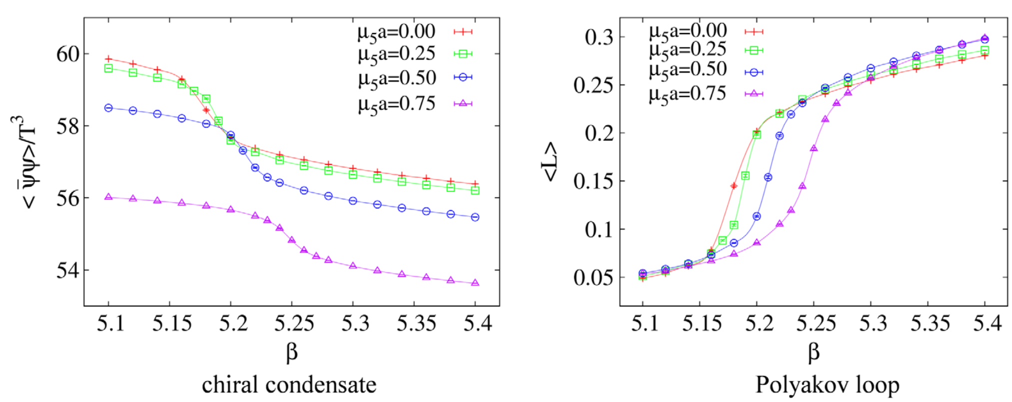

FIG. 1. Chiral condensate and Polyakov loop vs β for four values of $\mu_5 a$. The lattice size is 4×16^3, and the hopping parameter is $\kappa = 0.1665$. Errors are smaller than the data point symbols. The curves are to guide the eye.

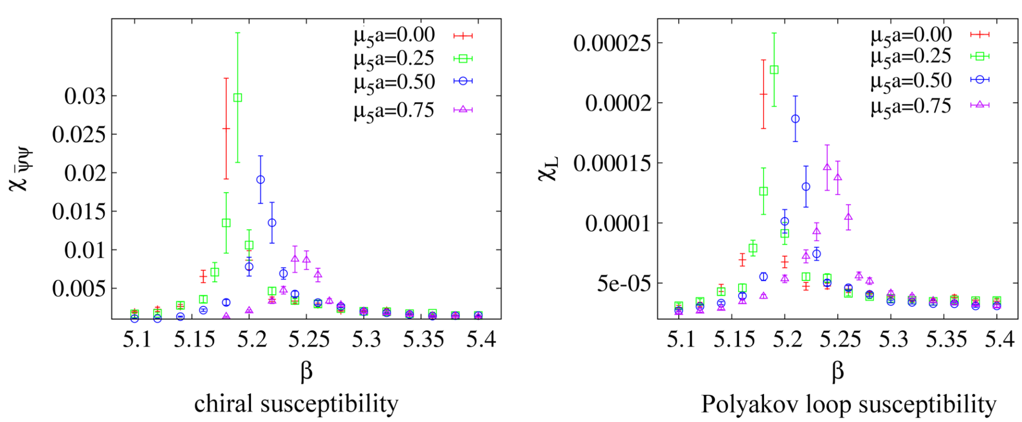

FIG. 2. Chiral susceptibility and Polyakov loop susceptibility vs β for four values of $\mu_5 a$. The lattice size is 4×16^3, and the hopping parameter is $\kappa = 0.1665$.

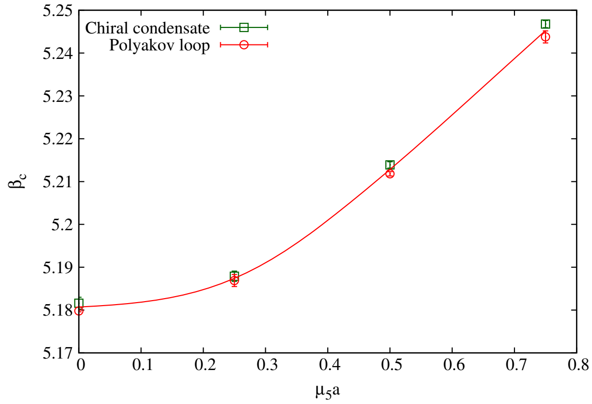

FIG. 3. Critical β_c for the chiral condensate and the Polyakov loop vs $\mu_5 a$. The lattice size is 4×16^3, and the hopping parameter $\kappa = 0.1665$. The curve is to guide the eyes.

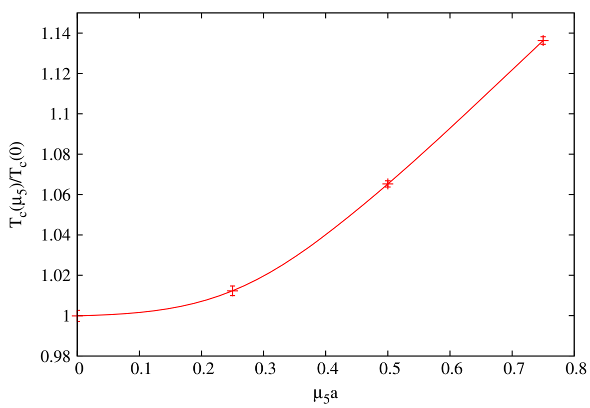

FIG. 4. Critical temperature $T_c(\mu_5)/T_c(0)$ for the chiral condensate vs $\mu_5 a$. The lattice size is 4×16^3, and the hopping parameter is $\kappa = 0.1665$. The curve is to guide the eyes.

and show that there are no additional divergences due to $\mu_5 \neq 0$ for Wilson fermions in the polarization operator. This implies that there are no additional divergences in the Polyakov loop.

Now it is important to discuss how nonzero chiral chemical potential affects scale setting in our simulations. The dependence of the coupling constant g^2 on the lattice spacing a is determined by the β-function. In perturbation theory the β-function can be calculated from the divergences of some Feynman diagrams. It is important to note that these divergences are logarithmic $\sim(\log a)^k$ due to gauge invariance. Now let us introduce the chiral chemical potential into the fermion propagators of the Feynman diagrams which contribute to the β-function. Evidently in the ultraviolet region one can expand the propagators in powers of μ_5. Since μ_5 has dimension of energy, beginning from the next-to-leading term in the μ_5 expansion the ultraviolet behavior of the Feynman diagrams becomes softer, and logarithmic divergences disappear. For this reason we believe that there are no additional contributions due to nonzero μ_5 in the β-function.

In the Appendix we present an analytical calculation of additional divergences in the chiral condensate for free Wilson fermions. The results of this study allow us to state that there are two additional divergences due to $\mu_5 \neq 0$: the first one is logarithmic, $\sim\mu_5^2 \log(a)$, and the second one is linear, $\sim\mu_5^2/a$. The logarithmic divergence also exists in the case of staggered fermions [31] with the same coefficient. The linear divergence is new as compared to staggered fermions. We believe that the linear divergence in the chiral condensate appears due to the explicit chiral symmetry breaking of Wilson fermions. Note that the coefficient in front of the linear divergence is negative. So, an increase of the chiral chemical potential leads to a decrease of the chiral condensate. It seems that this behavior persists in the interacting case. From Fig. 1 one sees that the curves with larger μ_5 are shifted down compared to the curves with smaller μ_5.

Despite the fact that the additional divergences due to $\mu_5 \neq 0$ give a considerable contribution to the value of the chiral condensate, we believe that there is no influence of the divergences to the position of the breaking/restoration chiral symmetry transition for the following reasons. First, as was noted above there are no divergences in the Polyakov loop. So, if additional divergences had influenced the position of the chiral symmetry breaking/restoration transition, it would be visible as a splitting between the chiral symmetry breaking/restoration and the confinement/deconfinement transitions. But we do not see such splitting. Notice also that the position of the phase transition manifests itself as a peak of the susceptibility. Evidently, there is no peak due to the additional ultraviolet divergence. All this allows us to state that the conclusions obtained in this paper are not affected by the additional ultraviolet μ_5 divergence in the chiral condensate.

IV. CONCLUSIONS

In this paper we have studied the phase diagram of $SU(3)$-QCD with a chiral chemical potential within lattice simulations using $N_f = 2$ flavors of dynamical Wilson fermions. We have calculated the chiral condensate, the Polyakov loop, the Polyakov loop susceptibility, and the chiral susceptibility for different values of the temperature T and the chiral chemical potential μ_5 on lattices of size 4×16^3. The main result is that at nonzero values of the chiral chemical potential, the critical temperatures of the confinement/deconfinement phase transition, and the chiral-symmetry breaking/restoration phase transition still coincide and that the common transition is shifted to larger temperatures as μ_5 increases.

In the present paper we have reported the first investigation of the phase diagram of $SU(3)$-QCD with a nonvanishing chiral chemical potential. In the following, one should extrapolate to physical quark masses and to the continuum limit in the hope to confirm the results. This exploration requires much larger computational resources and remains a task for future studies.

Our result is in agreement with a lattice study of the phase diagram of $SU(2)$-QCD [30,31]. Notice that the simulation described in Refs. [30,31] was carried out with staggered fermions which in the continuum corresponds to $N_f = 4$ flavors. A chiral chemical potential was introduced to the lattice action as an additive term. So, simulations with different fermion discretization and different numbers of colors and flavors give similar results. We believe that this is an argument in favor of the statement that the critical temperature of QCD-like systems rises as the chiral chemical potential is increased.

The studies of the QCD phase diagram with a chiral chemical potential within different effective models have given controversial results. For instance, the authors of Refs. [33–39] have predicted that the transition shifts to smaller temperatures as μ_5 increases. At the same time, some of the results obtained in Refs. [40,41] imply that the transition shifts to larger temperatures as μ_5 increases. In Ref. [41] it was shown that the results of effective models crucially depend on finer details of the models.

In Ref. [42] the influence of the chiral chemical potential on the chiral symmetry breaking/restoration transition was studied. It was shown that the chiral chemical potential enhances the chiral symmetry breaking and shifts the critical temperature to larger values. The result of our paper confirms this statement.

Besides effective models, the phase diagram of QCD in the (μ_5, T)-plane was studied in Refs. [43,44] in the framework of Dyson-Schwinger equations. We would like also to mention Ref. [45]. In this paper the authors address the question of universality of phase diagrams in QCD and QCD-like theories through the large-N_c equivalence. The authors of these papers found that the critical temperature rises with μ_5. These results agree with ours.

ACKNOWLEDGMENTS

The simulations were performed at the ITEP supercomputer. The work was supported by the Far Eastern Federal University, the Dynasty Foundation, by RFBR Grants No. 14-02-01185-a, No. 15-02-07596-a, and No. 15-32-21117 and by a grant of the FAIR-Russia Research Center.

APPENDIX: ULTRAVIOLET DIVERGENCES IN THE CHIRAL CONDENSATE

The fermion propagator including the chiral chemical potential for Wilson fermions can be written in the following form:

$$
\begin{aligned}
S^{\alpha\beta}(x,y) &= \frac{\delta^{\alpha\beta}}{L_t L_s^3}\sum_{\{k\}}\sum_{s=\pm1} e^{ip(x-y)} \frac{m+\frac{\hat{k}^2}{2} - i\sum_{i=1}^{3}\gamma_i \sin k_i - i\gamma_4 \sin k_4 \cosh\mu_5 - \cos k_4 \sinh\mu_5\gamma_4\gamma_5}{(m+\frac{\hat{k}^2}{2})^2 + \sin^2 k_4 \cosh^2\mu_5 + (|\bar{\mathbf{k}}| + s\cos k_4 \sinh\mu_5)^2} P(s),\\
P(s) &= \frac{1}{2}\left(1 - is\sum_{i=1}^{3}\frac{\gamma_i \sin k_i}{|\bar{\mathbf{k}}|}\gamma_4\gamma_5\right),\\
\bar{k}_\mu &= \sin k_\mu, \qquad \mu = 1,2,3,4,\\
|\bar{\mathbf{k}}| &= \sqrt{\sin^2 k_1 + \sin^2 k_2 + \sin^2 k_3},\\
\hat{k}_\mu &= 2\sin(k_\mu/2), \qquad \mu = 1,2,3,4,\\
\hat{k}^2 &= \sum_{\mu=1}^{4}\hat{k}_\mu^2,\\
k_i &= \frac{2\pi}{L_s}n_i, \qquad i = 1,2,3, \qquad n_i = 0,\ldots,L_s-1,\\
k_4 &= \frac{2\pi}{L_t}n_4 + \frac{\pi}{L_t}, \qquad n_4 = 0,\ldots,L_t-1.
\end{aligned}
\tag{A1}
$$

Here m and μ_5 are the mass and chiral chemical potential in lattice units, α and β are color indices, and the sum is taken over all possible values of (n_1, n_2, n_3, n_4). The relation between mass m and hopping parameter κ in our case is $\kappa = \frac{1}{2m+8}$

In the limit L_s, $L_t \to \infty$ the condensate can be written as

$$
\langle\bar{\psi}\psi\rangle = \mathrm{Tr}[S(x,x)] = 6\int_{-\pi}^{\pi}\frac{d^4k}{(2\pi)^4}\sum_{s=\pm1}\frac{m+\frac{\hat{k}^2}{2}}{(m+\frac{\hat{k}^2}{2})^2 + \sin^2 k_4\cosh^2\mu_5 + (|\bar{\mathbf{k}}| + s\cos k_4\sinh\mu_5)^2}. \tag{A2}
$$

To calculate the integral in formula (A2) we use the algebraic method, explained in Refs. [46,47]. The Taylor expansion in μ_5 tends to

$$\frac{1}{6}\langle\bar{\psi}\psi\rangle = 2\int_{-\pi}^{\pi}\frac{d^4k}{(2\pi)^4}\left[\frac{m+\frac{\hat{k}^2}{2}}{(m+\frac{\hat{k}^2}{2})^2+\sum_\mu \bar{k}_\mu^2} + \mu_5^2\left(-\frac{2(m+\frac{\hat{k}^2}{2})}{((m+\frac{\hat{k}^2}{2})^2+\sum_\mu \bar{k}_\mu^2)^2} + \frac{8\cos^2 k_4|\bar{\mathbf{k}}|^2(m+\frac{\hat{k}^2}{2})}{((m+\frac{\hat{k}^2}{2})^2+\sum_\mu \bar{k}_\mu^2)^3}\right)\right] + O(\mu_5^4). \quad \text{(A3)}$$

The first term in this expression is just the loop integral for $\langle\bar{\psi}\psi\rangle$ without chiral chemical potential. The expression for this integral in the limit $a \to 0$ can be written as follows:

$$2\int_{-\pi}^{\pi}\frac{d^4k}{(2\pi)^4}\frac{m+\frac{\hat{k}^2}{2}}{(m+\frac{\hat{k}^2}{2})^2+\sum_\mu \bar{k}_\mu^2} = c_0 + c_1 m + c_2 m^2 + m^3\left(\frac{\log m^2}{8\pi^2}+c_3\right) + O(m^4)$$

$$c_0 = 0.469363, \quad c_1 = -0,067967,$$
$$c_2 = -0,023613, \quad c_3 = -0,075829. \quad \text{(A4)}$$

The second term in (A3) we can calculate similarly. The result of the calculation can be written as follows:

$$\int_{-\pi}^{\pi}\frac{d^4k}{(2\pi)^4}\left(-\frac{2(m+\frac{\hat{k}^2}{2})}{((m+\frac{\hat{k}^2}{2})^2+\sum_\mu \bar{k}_\mu^2)^2} + \frac{8\cos^2 k_4|\bar{\mathbf{k}}|^2(m+\frac{\hat{k}^2}{2})}{((m+\frac{\hat{k}^2}{2})^2+\sum_\mu \bar{k}_\mu^2)^3}\right) = c_4 + m\left(-\frac{\log m^2}{4\pi^2}+c_5\right) + O(m^2)$$

$$c_4 = -0.010738, \quad c_5 = 0,045999. \quad \text{(A5)}$$

We have checked the last two formulas numerically. Restoring the lattice spacing a in our results we get

$$\langle\bar{\psi}\psi\rangle = \frac{6c_0}{a^3} + \frac{6c_1 m}{a^2} + \frac{6c_2 m^2}{a} + m^3\left(\frac{3\log(ma)}{2\pi^2}+6c_3\right) + \frac{6c_4\mu_5^2}{a} + \mu_5^2 m\left(-\frac{3\log(ma)}{\pi^2}+6c_5\right). \quad \text{(A6)}$$

The first line in formula (A6) represents the chiral condensate without chiral chemical potential, whereas the second line is the contribution due to nonzero μ_5. It is seen that there is an additional logarithmic divergence due to $\mu_5 \neq 0$. The same divergence with the same coefficient appears in the case of staggered fermions [31]. However, there is also a linear divergence $\sim\mu_5^2/a$ which is absent in the case of staggered fermions. We believe that this linear divergence in the chiral condensate appears due to the explicit chiral symmetry breaking of Wilson fermions. Note that the coefficient in front of the linear divergence is negative. So, an increase of the chiral chemical potential leads to a decrease of the chiral condensate that is seen in Fig. 1.

[1] D. E. Kharzeev, L. D. McLerran, and H. J. Warringa, Nucl. Phys. **A803**, 227 (2008).
[2] V. Skokov, A. Yu. Illarionov, and V. Toneev, Int. J. Mod. Phys. A **24**, 5925 (2009).
[3] A. Bzdak and V. Skokov, Phys. Lett. B **710**, 171 (2012).
[4] L. McLerran and V. Skokov, Nucl. Phys. **A929**, 184 (2014).
[5] S. L. Adler, Phys. Rev. **177**, 2426 (1969).
[6] J. S. Bell and R. Jackiw, Nuovo Cimento A **60**, 47 (1969).
[7] W. A. Bardeen, Nucl. Phys. **B75**, 246 (1974).
[8] D. E. Kharzeev, Annu. Rev. Nucl. Part. Sci. **65**, 193 (2015).
[9] E. Witten, Nucl. Phys. **B156**, 269 (1979).
[10] G. Veneziano, Nucl. Phys. **B159**, 213 (1979).
[11] V. G. Bornyakov, E. M. Ilgenfritz, B. V. Martemyanov, V. K. Mitrjushkin, and M. Müller-Preussker, Phys. Rev. D **87**, 114508 (2013).
[12] M. I. Buchoff *et al.*, Phys. Rev. D **89**, 054514 (2014).
[13] S. Sharma, V. Dick, F. Karsch, E. Laermann, and S. Mukherjee, *Proc. Sci.*, LATTICE2013 (2014) 164.
[14] S. Aoki, H. Fukaya, and Y. Taniguchi, Phys. Rev. D **86**, 114512 (2012).
[15] G. Cossu, S. Aoki, H. Fukaya, S. Hashimoto, T. Kaneko, H. Matsufuru, and J.-I. Noaki, Phys. Rev. D **87**, 114514 (2013); **88**, 019901(E) (2013).
[16] B. B. Brandt, A. Francis, H. B. Meyer, H. Wittig, and O. Philipsen, *Proc. Sci.*, LATTICE2012 (2012) 073.
[17] B. B. Brandt, A. Francis, H. B. Meyer, O. Philipsen, and H. Wittig, *Proc. Sci.*, LATTICE2013 (2014) 162.
[18] E. M. Ilgenfritz, B. V. Martemyanov, and M. Müller-Preussker, Phys. Rev. D **89**, 054503 (2014).
[19] D. E. Kharzeev, J. Liao, S. A. Voloshin, and G. Wang, arXiv:1511.04050.
[20] A. V. Sadofyev and Y. Yin, J. High Energy Phys. 01 (2016) 052.
[21] K. Rajagopal and A. V. Sadofyev, J. High Energy Phys. 10 (2015) 018.
[22] M. D'Elia, S. Mukherjee, and F. Sanfilippo, Phys. Rev. D **82**, 051501 (2010).
[23] G. S. Bali, F. Bruckmann, G. Endrodi, Z. Fodor, S. D. Katz, S. Krieg, A. Schafer, and K. K. Szabo, J. High Energy Phys. 02 (2012) 044 (2012).

[24] E. M. Ilgenfritz, M. Kalinowski, M. Müller-Preussker, B. Petersson, and A. Schreiber, Phys. Rev. D **85**, 114504 (2012).
[25] J. O. Andersen, W. R. Naylor, and A. Tranberg, arXiv:1411.7176.
[26] V. V. Braguta, A. Yu. Kotov, A. A. Nikolaev, and S. N. Valgushev, Proc. Sci., LATTICE2015 (**2016**) 186.
[27] V. V. Braguta, A. Yu. Kotov, A. A. Nikolaev, and S. N. Valgushev, Pis'ma Zh. Eksp. Teor. Fiz. **101**, 827829 (2015); [JETP Lett. **101**, 732 (2015)].
[28] S. Cotter, P. Giudice, S. Hands, and J.-I. Skullerud, Phys. Rev. D **87**, 034507 (2013).
[29] A. Yamamoto, Lect. Notes Phys. **871**, 387 (2013).
[30] V. V. Braguta, V. A. Goi, M. Ilgenfritz, A. Yu. Kotov, A. V. Molochkov, and M. Müller-Preussker, Pis'ma Zh. Eksp. Teor. Fiz. **100**, 623 (2015); [JETP Lett. **100**, 547 (2015)].
[31] V. V. Braguta, V. A. Goy, E. M. Ilgenfritz, A. Yu. Kotov, A. V. Molochkov, M. Müller-Preussker, and B. Petersson, J. High Energy Phys. 06 (2015) 094.
[32] A. Yamamoto, Phys. Rev. Lett. **107**, 031601 (2011).
[33] K. Fukushima, M. Ruggieri, and R. Gatto, Phys. Rev. D **81**, 114031 (2010).
[34] M. N. Chernodub and A. S. Nedelin, Phys. Rev. D **83**, 105008 (2011).
[35] R. Gatto and M. Ruggieri, Phys. Rev. D **85**, 054013 (2012).
[36] J. Chao, P. Chu, and M. Huang, Phys. Rev. D **88**, 054009 (2013).
[37] L. Yu, H. Liu, and M. Huang, Phys. Rev. D **90**, 074009 (2014).
[38] P. V. Buividovich, Phys. Rev. D **90**, 125025 (2014).
[39] P. V. Buividovich, M. Puhr, and S. N. Valgushev, Phys. Rev. B **92**, 205122 (2015).
[40] A. A. Andrianov, D. Espriu, and X. Planells, Eur. Phys. J. C **74**, 2776 (2014).
[41] L. Yu, H. Liu, and M. Huang, arXiv:1511.03073.
[42] V. V. Braguta and A. Yu. Kotov, arXiv:1601.04957.
[43] B. Wang, Y.-L. Wang, Z.-F. Cui, and H.-S. Zong, Phys. Rev. D **91**, 034017 (2015).
[44] S.-S. Xu, Z.-F. Cui, B. Wang, Y.-M. Shi, Y.-C. Yang, and H.-S. Zong, Phys. Rev. D **91**, 056003 (2015).
[45] M. Hanada and N. Yamamoto, *Proc. Sci.*, LATTICE2011 (2011) 221.
[46] G. Burgio, S. Caracciolo, and A. Pelissetto, Nucl. Phys. **B478**, 687 (1996).
[47] S. Capitani, Phys. Rep. **382**, 113 (2003).